18èmes Journées Internationales de Thermique (JITH 2017)
Monastir (Tunisie), 25 - 27 Octobre 2017

Parametric study of coupled heat and mass transfers in a cylinder filled with granular medium

Leila Zili-Ghedira, Boutheina Zallama, Sassi Ben Nasrallah
Université de Monastir, École Nationale d'Ingénieurs de Monastir, Laboratoire LESTE, Avenue Ibn El Jazzar 5019, Monastir, TUNISIE
leilazilighedira@yahoo.fr, zallama.boutheina@live.fr, Sassi.Bennasrallah@enim.rnu.tn,

Abstract:
In this paper heat and mass transfers and forced convection fluid flow within a cylindrical saturated granular medium are studied numerically. The used model is an unsteady two-temperature one accounting for variable porosity. The selected medium is silica gel. The study focuses on the effects of the whether parameters i e air temperature and humidity and also the geometric parameters i e form factor of the cylinder. It is deduced that the bed adsorption can be improved by considering lower air temperature and form factor and higher air absolute humidity.

Keywords : numerical study, granular medium, saturated medium, parametric analysis.

1. Introduction

The attention given to the improvement of the various industrial systems is growing in the aim of both reducing energy consumption and improving their performance. Then heat and mass transfers and fluid flow through granular medium is essential to optimize the functioning of several systems in the area of buildings thermal insulation, engineering oil, refrigeration machines, desiccant cooling air systems, …

Indeed this research is aimed at the comprehension and optimization of the fluid flow and heat and mass transfers in a cylindrical packed bed filled with a saturated porous medium.

In literature several papers deal with the adsorption phenomenon in porous media. Both numerical and experimental studies are encountered.

A numerical study was conducted by Solmus et al [1]. It was aimed to exploring the fields of temperature, pressure and to evaluate the adsorbed steam rate in a cylindrical packed bed filled with silica gel and subjected to a radial flow. The used model is a transient one-dimensional non-equilibrium temperature one. It is shown that reducing intra-particle thermal transfer resistances and mass transfer resistances improves bed performances.

White [2] developed a Computational Fluid Dynamics model dedicated to the study of the adsorption phenomenon in silica gel bed. The main outcome of this study is that the adsorption rate is enhanced when reducing the particles' size.

Ramzy et al. [3] simulated numerically transfers in a desiccant bed. In this study, two models were compared: one mathematical model based on the strength of solid side and another based on the strength of the solid side and considering the heat conduction along the bed. It was concluded that in order to reduce the axial heat conduction along the bed, the particle diameter and the air flow rate should be increased and the bed thickness should be decreased.

Chang et al. [4] explored experimentally a bed filled with metal substrate covered with silica gel. It was observed that the adsorption capacity is enhanced for lower adsorbent thickness and higher particle diameters.

Niazmand et al. [5] explored a finned tubes heat exchanger with mesoporous silica gel. A specific particle diameter was demonstrated optimal for the porous bed performance; in fact the inter- and intra-particle mass transfer resistances effects are opposite. This optimal particle size is proven to depend on the fins height and spacing and on the cooling/heating temperatures.

The performance of a new composite formed by silica gel and natural graphite treated with sulfuric acid was conducted by Zheng et al. [6] via experiments on different silica gel percentages. It was shown that the thermal conductivity is inversely proportional to the percentage of silica gel.

From this literature survey, it can be drawn back that the used numerical models rely on the assumptions of stationary regime, one-dimensional flow and constant porosity.

This solicits the present numerical contribution via an unsteady, two-temperature, two-dimensional model with variable porosity. In addition, the parameters effects discussed here weren't explored in literature. An analysis dedicated to the effects of whether parameters and geometric parameters on a silica gel bed was conducted: the effects of air temperature and absolute humidity and form factor were discussed.

2. Mathematical formulation

The study concerns a cylinder containing a granular saturated medium. The used model is a transient two-dimensional one. It was developed and validated in a previous work (Zili and Ben Nasrallah [7]).

In this work it is assumed that the fluid is a Newtonian perfect gas with constant physical properties, the medium is isotropic, the radiation is neglected and the flow is not affected by the heat and mass transfers so the flow equations are solved at first generating a velocity field injected to solve heat and mass transfers [8].

2.1. Flow formulation

It is based on the Darcy-Brinkman-Forchheimer law [9].

2.1.1. Continuity equation

$$\frac{\partial \mathrm{v_z}}{\partial z}+\frac{1}{r}\frac{\partial}{\partial r}\left(r\ v_r\right)=0 \tag{1}$$

2.1.2. Momentum equation

$$\frac{1}{\varepsilon}\left(v_z\frac{\partial \mathrm{v_z}}{\partial z}+v_r\frac{\partial \mathrm{v_z}}{\partial \mathrm{r}}\right)=-\frac{1}{\rho_f}\frac{d\mathrm{P}}{\mathrm{dz}}+\frac{1}{\rho_f}\frac{1}{r}\frac{\partial}{\partial r}\left(r\mu_f\frac{\partial \mathrm{v_z}}{\partial r}\right)-\frac{\varepsilon v_f}{K}v_z-\frac{\varepsilon F}{\mathrm{K}^{1/2}}{v_z}^2 \tag{2}$$

2.2. Heat and mass transfers' formulation

2.2.1. Vapour and air mass conservation equations

$$\varepsilon\frac{\partial \rho_\mathrm{v}}{\partial t}+\frac{1}{r}\frac{\partial}{\partial r}\left(r\rho_\mathrm{v}v_\mathrm{r}\right)+\frac{\partial\left(\rho_\mathrm{v}v_\mathrm{z}\right)}{\partial z}=\dot{M}+\frac{\partial}{\partial z}\left(\rho_\mathrm{f}D_\mathrm{effz}\frac{\partial}{\partial z}\left(\frac{\rho_\mathrm{v}}{\rho_\mathrm{f}}\right)\right)+\frac{1}{r}\frac{\partial}{\partial r}\left(r\rho_\mathrm{f}D_\mathrm{eff,r}\frac{\partial}{\partial r}\left(\frac{\rho_\mathrm{v}}{\rho_\mathrm{f}}\right)\right) \tag{3}$$

where $\dot{M}$ is the average rate of water evaporation.

$$\dot{M}=-(1-\varepsilon)\rho_{sd}\frac{\partial X}{\partial t} \tag{4}$$

D_{eff} is the effective diffusivity expressed, respectively, in the axial and radial directions as [10] :

$$D_{\mathrm{eff,z}}=0.7\,D+0.5\,D\,Pe^{1.2}$$

$$D_{\mathrm{eff,r}}=0.7\,D+0.01\,D\,Pe^{0.9}$$

where D is the molecular diffusivity and Pe is the Peclet number.

$$\varepsilon\frac{\partial \rho_\mathrm{a}}{\partial t}+\frac{1}{r}\frac{\partial}{\partial r}\left(r\rho_\mathrm{a}v_\mathrm{r}\right)+\frac{\partial\left(\rho_\mathrm{a}v_\mathrm{z}\right)}{\partial z}=\frac{\partial}{\partial z}\left(\rho_\mathrm{f}D_\mathrm{eff,z}\frac{\partial}{\partial z}\left(\frac{\rho_\mathrm{a}}{\rho_\mathrm{f}}\right)\right)+\frac{1}{r}\frac{\partial}{\partial r}\left(r\rho_\mathrm{f}D_\mathrm{eff,r}\frac{\partial}{\partial r}\left(\frac{\rho_\mathrm{a}}{\rho_f}\right)\right) \tag{5}$$

2.2.2. Energy conservation equation in the gaseous and solid phases

$$\frac{\partial}{\partial t}\left(\varepsilon\rho_f C_{p_f} T_f\right)+\frac{1}{r}\frac{\partial}{\partial r}\left(r\rho_f v_r C_{p_f} T_f\right)+\frac{\partial}{\partial z}\left(\rho_f v_z C_{pf} T_f\right)$$
$$=H_{fs} s\left(T_{sd}-T_f\right)+\dot{M} C_{p_v} T_{sd}+\frac{1}{r}\frac{\partial}{\partial r}\left(r\lambda_{eff,r}\frac{\partial T_f}{\partial r}\right)+\frac{\partial}{\partial z}\left(\lambda_{eff,z}\frac{\partial T_f}{\partial z}\right) \quad (6)$$

The gas effective conductivity in the axial and radial directions is expressed by [11, 12]:

$$\lambda_{effz}=\varepsilon\lambda_f+0.5\left[\Pr\left(\frac{\rho_f v_z d}{\mu_f}\right)\right]\lambda_f ,$$

$$\lambda_{effr}=\varepsilon\lambda_f+0.1\left[\Pr\left(\frac{\rho_f v_z d}{\mu_f}\right)\right]\lambda_f ,$$

where λ_f represents the gas conductivity.

$$\left(1-\varepsilon\right)\rho_{sd}\left(C_{sd}+XC_w\right)\frac{\partial T_{sd}}{\partial t}=H_{fs} s\left(T_f-T_{sd}\right)+\frac{1}{r}\frac{\partial}{\partial r}\left(r\lambda_{eff,s}\frac{\partial T_{sd}}{\partial r}\right)+\frac{\partial}{\partial z}\left(\lambda_{eff,s}\frac{\partial T_{sd}}{\partial z}\right)-\dot{M}\,\Delta h_{ads} \quad (7)$$

where $\Delta h_{ads}=\Delta h^0{}_{ads}+\left(C_{pv}-C_w\right)T_s$ and $\Delta h^0{}_{ads}=\left(h_v^0-h_w^0\right)+\left(C_w-C_{p_v}\right)T_0$

The effective solid conductivity is [12]:

$$\lambda_{eff,s}=\left(1-\varepsilon\right)\lambda_{sd}$$

where λ_{sd} represents the solid conductivity.

2.2.3. Adsorption kinetics

The amount of adsorbate contained in the adsorbent at equilibrium (Freundlish [13]) is:

$$X_\infty = 0.24\,\varphi^{1/1.5} \quad (8)$$

where φ is the air relative humidity.

The adsorption kinetics [1, 13-15] is:

$$\frac{\partial X}{\partial t} = k_m\,(X_\infty - X) \quad (9)$$

where $k_m = 15\, D_e/{r_p}^2$ *and* $D_e = D_o exp\,(-E_a/R\,T_{sd})$

The used parameters are: $D_o = 2.54\ 10^{-4}\ m^2\ s^{-1}$ and $E_a = 4.2\ 10^4\ J\ mol^{-1}$.

3. Numerical resolution

Flow equations and heat and mass transfer equations are solved separately [7, 16].

3.1. Numerical resolution

The flow equations resolution is done by the finite difference method [17]. A fully implicit method is used. The discretization is done by an iterative method. A uniform mesh is used.

The mass and heat transfers' equations resolution is done by the finite field method [17]. The used mesh is uniform and the calculation steps are constant. An implicit scheme is adopted. For convection terms Upwind scheme is used. Resolution is done by the line by line iterative method in the axial direction.

Convergence is reached when arbitrary fields and calculated solutions coincide within a relative error. Otherwise, the calculated fields will be taken as arbitrary and calculations will be resumed until convergence.

The code validation was conducted in a previous work [18].

3.2. Initial and boundary conditions

Initially, the medium is considered at the same temperature of the ambiance, and so the gas and solid temperatures. Dry air and vapour densities are also initially considered constant.

At the cylinder inlet gas temperature is equal to that of air blown through the bed, while for solid temperature a heat transfer coefficient is used [19, 20]. Concerning dry air and vapour densities at the bed entrance, they are adopted equal to those of the blown air.

At the cylinder outlet both heat transfer coefficients are adopted for gas and solid temperature and mass transfer coefficients are used for dry air and vapour densities [19, 20].

At the axis of the cylinder symmetry of revolution is considered.

The cylinder surface is taken insulated and impermeable.

4. Numerical simulation results

In simulation, the considered reactor is 0.15 m in radius and 0.05 m in height.

Water initial content in the medium is $x_i = 0.007$ kg of water/kg of dry product. Average grains diameter is $d = 3 .10^{-3} m$. Exchange surface per unit volume is $s = \frac{6(1-\varepsilon)}{d}$. Initial dry air and vapour densities are $\rho_{a_i} = 1.158519$ kg/m^3 and $\rho_{v_i} = 0.000167$ kg/m^3. Initial medium temperature and relative humidity are $T_i = 305$ °K and $\varphi_i = 0.5\%$.

Air densities, respectively, at the inlet/outlet are $\rho_{a_0} = 1.124732$ kg/m^3 and $\rho_{a_{00}} = 1.141490$ kg/m^3. Vapour densities, respectively, at the inlet/outlet are $\rho_{v_0} = 0.021139$ kg/m^3 and $\rho_{v_{00}} = 0.010737$ kg/m^3. Temperatures and relative humidities at the inlet and the outlet are $T_0 = T_{00} = 305$ °K and $\varphi_0 = 63\%; \varphi_{00} = 32\%$.

Gas thermal conductivity and dynamic viscosity are $\lambda_f = 0.026$ W/m.°K and $\mu_f = 1.5\ 10^{-5}$ kg/(m s).

A parametric study is conducted. This study explores the effects of the weather parameters (blown air temperature and absolute humidity) and the geometric parameters (form factor) on the adsorption phenomenon.

4.1. Weather parameters effect

From a literature survey concerning studies related to desiccator behavior, one can notice the missing of research dealing with weather effects on the adsorption. For this reason the present part is dedicated to elucidate the effects of air temperature and absolute humidity on the desiccator adsorption capacity.

4.1.1. Air temperature effect

The present section is dedicated to exploring the air temperature effect on the adsorption capacity.

FIG. 1 (a) and (b) is a representation, respectively, of the temporal evolution of temperature difference and relative humidity difference between the bed outlet and inlet. Three different values were tested by taking successively blown air temperature equal to 28°C, 32°C and 40°C.

FIG. 1 (b) relates an increase of the absolute value of the relative humidity difference when reducing the air temperature; from 37% for 40°C to 70% for 28°C. This reveals an increase in the adsorption capacity with the decrease of the air temperature.

On another side, the temperature difference between the bed inlet and outlet is sensibly the same for the three cases (FIG. 1 (a)) especially when viewing peaks of temperature differences. Otherwise, we may depict a very little increase of temperature difference between the desiccator outlet and inlet when decreasing the blown air temperature.

It follows that it remains well beneficial to reduce air temperature before blowing it through the reactor when targeting to improve desiccator capacity of adsorbing.

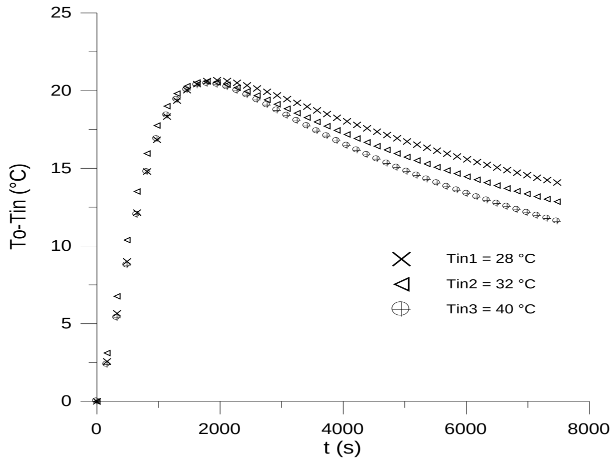

(a)

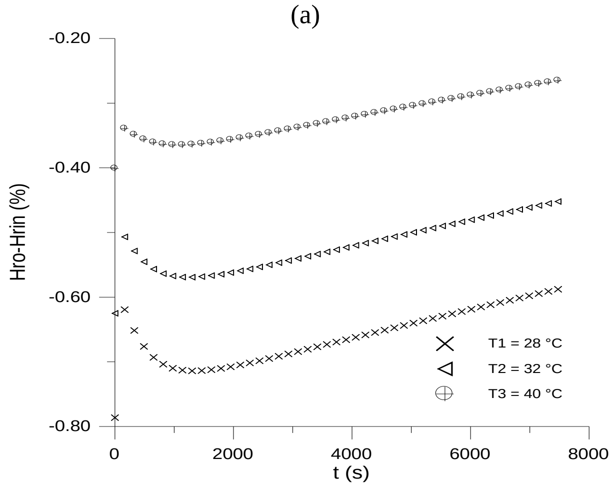

(b)

Figure 1: Air temperature effect on the adsorption phenomenon
(a) Temperature difference temporal evolution
(b) Relative humidity difference temporal evolution

4.1.2. Air absolute humidity effect

The effect of the air absolute humidity on adsorption capacity is tested in this section. For this aim, the temporal temperature difference and relative humidity difference between the bed outlet and inlet are respectively represented in FIG. 2 (a) and (b). The considered air absolute humidities are 12.815 g/kg, 20.511 g/kg and 22.073 g/kg.

The main outcome of these illustrations is the increase of the temperature difference and that of the absolute value of the relative humidity difference when increasing the air specific humidity.

This demonstrates an elevation of the adsorption capacity in regards with the air absolute humidity amplification.

Otherwise, the adsorption capacity enhancement results in an increase of the released heat due to the adsorption operation which is an exothermic process. Indeed, the adsorption capacity increase is dedicated to the elevation of the water vapour potential present in the blown air when increasing its absolute humidity.

These conclusions are quite clear in table 1 which represents the results for four different values of blown air absolute humidity. In fact, this table shows an increase of the absolute value of the air relative humidity difference outlet/inlet from 38% for blown air absolute humidity of 12.81 g/kg to 66% for 22.07 g/kg.

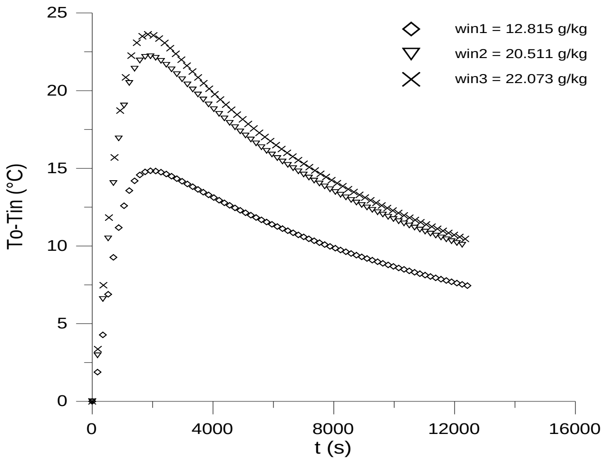

(a)

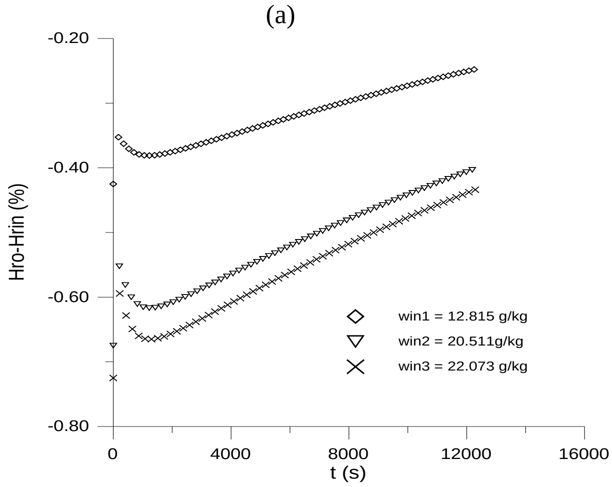

(b)

Figure 2: Absolute humidity effect on adsorption phenomenon
(a) Temporal temperature difference
(b) Temporal relative humidity difference

Table 1: Absolute humidity effect on the adsorption phenomenon characteristics

	Absolute humidity at the desiccator inlet *(g/kg)*			
	12.81	18.95	20.51	22.07
ΔHr*(%)*	38	57	62	66
ΔT *(°C)*	7.7	19.2	20.6	21.9

4.2. Geometric effects: Form factor effect

The form factor exhibits the geometric effects. In fact, it represents the cylinder diameter by height ratio.

The advanced effect is explored in this section by the consideration of three different values which are 1.11, 3.75 and 17.5. These values are adopted while maintaining the same air flow rate, air characteristics (temperature and relative humidity) and porous medium volume.

The results are represented in FIG. 3 (a) and (b), showing respectively temporal evolution of temperature and relative humidity at the desiccator exit.

The outcome of these tests is that the adsorption capacity is enhanced when reducing the form factor (FIG. 3 (b)); in this sense the figure relates a decrease of the air relative humidity at the desiccator exit. As a result the released heat by the adsorption phenomenon is increased as noticed in FIG 3 (a).

This behavior can be explained by the fact that the reduction of the form factor induces an increase of the air speed through the bed and then the increase of the gas-solid heat exchange coefficient resulting in enhancing exchange between adsorbent and adsorbate.

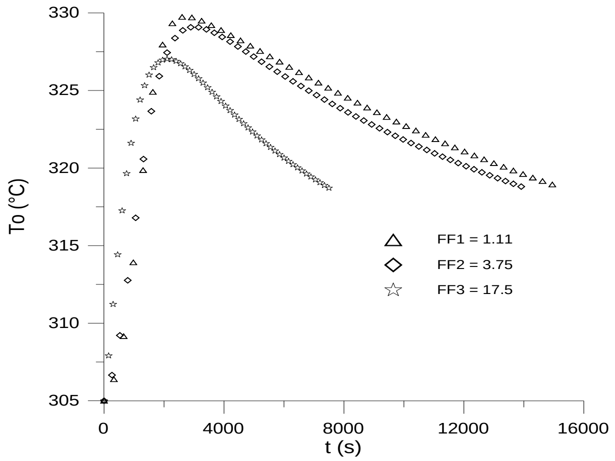

(a)

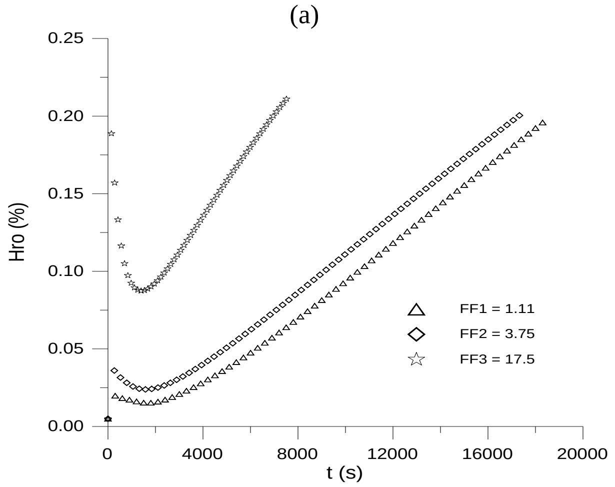

(b)

Figure 3: Form factor effect on the adsorption phenomenon
(a) Exit temperature temporal evolution
(b) Exit relative humidity temporal evolution

Conclusion

This paper exposes a mathematical model dedicated to the study of the flow and heat and mass transfers in a cylinder filled with a granular saturated medium. A numerical transient two-dimensional two-temperature code was proposed.

The study explores the different effects of varying the weather characteristics, i. e. blown air temperature and absolute humidity and geometric characteristics, i. e. form factor on the adsorption capacity.

It is depicted that higher air temperatures reduce adsorption capacity. Then it is advantageous to use different techniques such as cooling and heat storage to improve the adsorption process.

Air absolute humidity increase causes increase of vapour adsorbed amount given the available potential of the vapour present in the air.

The reduction of the form factor, thus, reducing the cylinder diameter per height ratio, results in adsorption capacity improvement owing to fluid acceleration (while the same flow rate is conserved).

Nomenclature

C specific heat, *J kg^{-1} K^{-1}*
C_p specific heat at constant pressure, *J kg^{-1} K^{-1}*
d average grain diameter, *m*
D diffusion coefficient for gaseous phase, *m^2 s^{-1}*
F Forchheimer coefficient
H_{fs} gas-solid exchange coefficient, *W m^{-2} K^{-1}*
K granular medium intrinsic permeability, *m^2*
$\dot{M}$ average adsorbed water rate within grains, *kg m^{-3} s^{-1}*
P intrinsic averaged pressure, *Pa*
Pe Peclet number
Pr Prandtl number
r radial coordinate, *m*
R constant of perfect gas, *J mol^{-1} K^{-1}*
r_p average particle radius, *m*
s gas-solid exchange surface per unit volume, *m^{-1}*
t time, *s*
T intrinsic averaged temperature, *K*
v average velocity, *m s^{-1}*
x granular medium water content, *kg of water . kg^{-1} of dried product*
z axial coordinate, *m*

Greek letters

Δh_{ads} averaged adsorption enthalpy, *J kg^{-1}*
ε granular medium porosity
λ conductivity, *W m^{-1} K^{-1}*
μ gas dynamic viscosity, *kg m^{-1} s^{-1}*
ν gas kinematics viscosity, *m^2 s^{-1}*
ρ intrinsic average density, *kg m^{-3}*

Subscripts

a air
eff, effr, effz gas effective, radial component, axial component
eff,s solid effective
f fluid
r radial
sd solid
v vapour
w water
z axial

References

[1] I. Solmus, D. A. S. Rees, C. Yamali, D. Baker and B. Kaftanoglu, Numerical investigation of coupled heat and mass transfer inside the adsorbent bed of an adsorption cooling unit, *Int. J. Refrigeration*, vol. 35, pp. 652-662, 2012.
[2] J. White, A CFD simulation on how the different sizes of silica gel will affect the adsorption performance of silica gel, *Model. Simul. Eng.*, vol 2012, pp. 8-20, 2012.
[3] K. A. Ramzy, R. Kadoli and T. P. Ashok Babu, Significance of axial heat conduction in nonisothermal adsorption process in a desiccant packed bed, *Int. J. Therm. Sciences*, vol. 76, pp. 68-81, 2014.
[4] K.-S. Chang, M.-T. Chen, T.-W. Chung, Effects of the thickness and particle size of silica gel on the heat and mass transfer performance of a silica gel-coated bed for air-conditioning adsorption systems, *Appl. Therm. Eng.*, vol. 25 (n°14–15), pp. 2330–2340, 2005.
[5] H. Niazmand, H. Talebian, M. Mahdavikhah, Effects of particle diameter on performance improvement of adsorption systems, *Appl. Therm. Eng.*, vol. 59, pp. 243–52, 2013.
[6] X. Zheng, L.W. Wang, R.Z. Wang, T.S. Ge, T.F. Ishugah, Thermal conductivity, pore structure and adsorption performance of compact composite silica gel, *Int. J. Heat Mass Transfer*, vol. 68, pp. 435–443, 2014.
[7] L. Zili, S. Ben Nasrallah, Heat and mass transfer during drying in cylindrical packed beds, *Numerical Heat Transfer*, Part A, vol. 36 (n°2), pp. 201-228, 1999.
[8] K. Vafai and CL. Tien, Boundary and Inertia effects on flow and heat transfer in porous media, *Int. J. Heat Mass Transfer*, vol. 108, pp. 195–203, 1981.
[9] C. T. Hsu and P. Cheng, Thermal dispersion in a porous medium, *Int. J. Heat Mass Transfer*, vol. 33, pp. 1587-1597, 1990.
[10] M. Sahimi, Flow and transport in porous media and fractured rock - From classical methods to modern approaches, Chap. 9, *Dispersion in porous media*, pp. 215-260, printed in the Federal Republic of Germany, 1995.
[11] A. Amiri and K. Vafai, Analysis of dispersion effects and non-thermal equilibrium, non-Darcian, variable porosity incompressible flow through porous media, *Int. J. Heat Mass Transfer*, vol. 37, pp. 939-954, 1994.
[12] M. L. Hunt et C. V. Le Tien, Non-Darcian convection in cylindrical packed beds, *ASME Journal of Heat Transfer*, vol. 110, pp. 378-384, 1988.
[13] A. Kodama, T. Hirayama, M. Goto, The use of psychrometric chart for the optimization of a thermal swing desiccant wheel, *Appl. Thermal Eng*, vol. 21, pp.1657–1674, 2001.
[14] M. H. Ahmed, N. Kattab, M. and M. Fouad, Evaluation and optimization of solar dessiccant wheel performance, *Ren. Energy*, vol. 30, pp. 305-325, 2005.

[15] A. Sakoda and M. Suziki, Simultaneous transport of heat and mass in closed type adsorption cooling system utilising solar heat, *J. Solar Energy Eng., ASME*, vol. 108, pp. 239-290, 1986.
[16] L. Zili- GHEDIRA, Etude des transferts de chaleur et de masse dans un milieu granulaire, thèse de doctorat, Université de Monastir, Ecole Nationale d'Ingénieurs de Monastir, Mars 2002.
[17] S. V.Patankar, Numerical heat transfer and fluid flow. In: Series in computational methods in mechanics and thermal sciences, Hemisphere publishing Corporation, New York, 1980.
[18] L. Zili-Ghedira, I. Mtimet and S. Ben Nasrallah, Performances of a Silica Gel Reactor within an Adsorption Cooling System**,** *J. Porous Media*, vol. 12(2), pp. 131-141, 2009.
[19] A. Mhimid and S. Ben Nasrallah, Theoretical study of heat and mass transfers during drying in granular products, in I. Turner and A. S. Mujumdar (eds.), *Mathematical modeling and numerical techniques in drying technology*, Marcel and Dekker, Inc.; New York, pp. 381-413, 1997.
[20] S. Ben Nasrallah, T.Amara and M. A. Peuty, Convection naturelle instationnaire dans un cylindre rempli de grains, ouvert à ses extrémités et dont la paroi est chauffée par un flux de chaleur constant: validité de l'hypothèse de l'équilibre thermique local, *Int. J. Heat Mass Transfer*, vol. 40, pp. 1155-1168, 1997.